

Complexity of switching chaotic maps in finite precision

M. Antonelli^{1,2}, L. De Micco^{1,2,3}, O. A. Rosso^{3,4,5,6} and H. A. Larrondo^{1,2,3}

¹ Facultad de Ingeniería, Universidad Nacional de Mar del Plata, Mar del Plata, Argentina.

² ICyTE. Instituto de Investigaciones Científicas y Tecnológicas en Electrónica.

³ CONICET. Consejo Nacional de Investigaciones Científicas y Técnicas

⁴ Departamento de Informática en Salud, Hospital Italiano de Buenos Aires, C1199ABB Ciudad Autónoma de Buenos Aires, Argentina.

⁵ Instituto de Física, Universidade Federal de Alagoas (UFAL), Maceió, Brazil.

⁶ Facultad de Ingeniería y Ciencias Aplicadas, Universidad de Los Andes, Santiago, Chile.

Abstract

In this paper we investigate the degradation of the statistic properties of chaotic maps as consequence of their implementation in a digital media such as Digital Signal Processors (DSP), Field Programmable Gate Arrays (FPGA) or Application-Specific Integrated Circuits (ASIC).

In these systems, binary floating- and fixed-point are the numerical representations available. Fixed-point representation is preferred over floating-point when speed, low power and/or small circuit area is necessary. The specific period that every fixed-point precision produces was investigated in previous reports, using as example the tent map and the logistic map [1]. After this, authors applies switching and skipping techniques to enlarge the periods.

Statistical characteristics are also relevant. It has been recently shown that it is convenient to describe the statistical characteristic using both, causal and non-causal quantifiers. In this paper we complement the period analysis by characterizing the behavior of these maps from an statistical point of view using causal and non-causal entropies and complexities.

VERSION: September 28, 2017

1 Introduction

In the last years digital systems became the standard in all experimental sciences. By using new programmable electronic devices such as DSP's and Reconfigurable electronics such as FPGA's or ASIC's, experimenters are allowed to design and modify their own signal generators, measuring systems, simulation models, etc.

When a chaotic system is implemented in computers or any digital device, the chaotic attractor become periodic by the effect of finite precision, then only pseudo chaotic attractors can be generated [2,3]. Discretization may even destroy the pseudo chaotic behavior and consequently is a non trivial process [4,5,6].

In these new devices, floating- and fixed-point are the available arithmetic. Floating-point is the more accurately solution but is not always recommended when speed, low power and/or small circuit area are required, a fixed-point solution is better in these cases.

The effect of numerical discretization over a chaotic map was recently addressed in [2] and [6]. In [2], author characterizes the Moire interfaces in the Mandelbrot system. These interfaces are consequence of precision data type and do not appear in the ideal system using real numbers. In [6], authors explore the statistical degradation of the phases' space for a family of 2D quadratic maps. These maps present a multiattractor dynamic that makes them very attractive as random number generator in fields like criptography, encoding, etc.

Grebogi and coworkers [7] studied this subject and they saw that the period T scales with roundoff ϵ as $T \sim \epsilon^{-d/2}$ where d is the correlation dimension of the chaotic attractor. To have a large period T is an important property of chaotic maps, in [1] Nagaraj *et. al* studied the effect of switching over the average period lengths of chaotic maps in finite precision. They saw that the period T of the compound map obtained by switching between two chaotic maps is higher than the period of each map. Liu *et. al* [8] studied different switching rules applied to linear systems to generate chaos. Switching issue was also addressed in [9], the author considered some mathematical, physical and engineering aspects related to singular, mainly switching systems. Switching systems naturally arise in power electronics and many other areas in digital electronics. They have also interest in transport problems in deterministic ratchets [10] and it is known that synchronization of the switching procedure affects the output of the controlled system.

Stochasticity and mixing are also relevant to characterize a chaotic behavior. To investigate these properties several quantifiers were studied [11]. Entropy

and complexity from information theory were applied to give a measure for causal and non causal entropy and causal complexity.

A fundamental issue is the criterium to select the probability distribution function (PDF) assigned to the time series, causal and non causal options are possible. Here we considered the non causal traditional PDF obtained by normalizing the histogram of the time series. Its statistical quantifier is the normalized entropy H_{hist} that is a measure of equiprobability among all allowed values. We also considered a causal PDF that is obtained by assigning ordering patterns to segments of trajectory of length D . This PDF was first proposed by Bandt & Pompe in a seminal paper [12]. The corresponding entropy H_{BP} was also proposed as a quantifier by Bandt & Pompe, in [13] authors applied the causal complexity C_{BP} to detect chaos. Among them the use of an entropy-complexity representation ($H_{hist} \times C_{BP}$ plane) and causal-non causal entropy ($H_{BP} \times H_{hist}$ plane) deserves special consideration [11,13,14,15,16,17,18].

Recently, amplitude information was introduced in [19] to add some immunity to weak noise in a causal PDF. The new scheme better tracks abrupt changes in the signal and assigns less complexity to segments that exhibit regularity or are subject to noise effects. Then, we define the causal entropy with amplitude contributions H_{BPW} and the causal complexity with amplitude contributions C_{BPW} . Also, we introduce the modified planes $H_{hist} \times C_{BP}$ and $H_{BP} \times H_{hist}$.

Amigó and coworkers proposed the number of forbidden patterns as a quantifier of chaos [20]. Essentially they report the presence of forbidden patterns as an indicator of chaos. Recently it was shown that the name forbidden patterns is not convenient and it was replaced by missing patterns (MP) [21], in this work authors show that there are chaotic systems that present MP from a certain minimum length of patterns. Our main interest on MP is because it gives an upper bound for causal quantifiers.

Following [1], in this paper we study the statistical characteristics of five maps, two well known maps: (1) the tent (TENT) and (2) logistic (LOG) maps, and three additional maps generated from them: (3) SWITCH, generated by switching between TENT and LOG; (4) EVEN, generated by skipping all the elements in odd positions of SWITCH time series and (5) ODD, generated by discarding all the elements in even positions of SWITCH time series. Binary floating- and fixed-point numbers are used, these specific numerical systems may be implemented in modern programmable logic devices.

The main contributions of this paper are:

- (1) the definition of different statistical quantifiers and their relationship with the properties of the time series generated by the studied chaotic maps.
- (2) the study of how these quantifiers detect the evolution of stochasticity and mixing of the chaotic maps according as the numerical precision varies.

- (3) the effect on the period and the statistical properties of the time series of switching between two different maps.
- (4) the effect on the period and the statistical properties of the time series of skipping values in the switched maps.

Organization of the paper is as follows: Section 2 describes the statistical quantifiers used in the paper and the relationship between their value and the characteristics of the causal and non causal PDF's considered; Section 3 shows and discusses the results obtained for all the numerical representations. Finally Section 4 deals with final remarks and future work.

2 Information theory quantifiers

Dynamical systems are systems that evolve in time. In practice, one may only be able to measure a scalar time series $X(t)$ which may be a function of variables $V = \{v_1, v_2, \dots, v_k\}$ describing the underlying dynamics (i.e. $dV/dt = f(V)$). We try to infer properties of an unfamiliar system from the analysis of measured record of observational data. How much information are these data revealing about the dynamics of the underlying system or processes? The information content of a system is typically evaluated via a probability distribution function (PDF) P describing the apportionment of some measurable or observable quantity, generally a time series $X(t)$. We can define Information Theory quantifiers as measures able to characterize relevant properties of the PDF associated with these time series, and in this way we should judiciously extract information on the dynamical system under study. These quantifiers represent metrics on the space of PDFs for data sets, allowing to compare different sets and classifying them according to their properties of underlying processes, broadly, stochastic vs. deterministic.

In our case, we are interested in chaotic dynamics. Thus we are focused in metrics which take the temporal both order of observations explicitly into account; i.e. the approach is fundamentally *causal* and *statistical* in nature. In a purely statistical approach, correlations between successive values from the time series are ignored or simply destroyed via construction of the PDF; while a causal approach focuses on the PDFs of data sequences.

The selected quantifiers are based on symbolic counting and ordinal pattern statistics. The metrics to be used can be broadly classified along two categories: those which quantify the *information content* of data versus those related to their *complexity*. Note that, here we are referring to the space of probability density functions, not physical space. For the sake of clarity and simplicity, we only introduce Information Theory quantifiers that are defined on discrete PDFs in this section, since we are only dealing with discrete data (time series).

However, all the quantifiers also have definitions for the continuous case [22].

2.1 Shannon entropy and statistical complexity

Entropy is a basic quantity that can be regarded to as a measure of the uncertainty associated (information) to the physical process described by P . When dealing with information content, the Shannon entropy is often considered as the foundational and most natural one [22]. Regarded as a measure of uncertainty, is the most paradigmatic example of these information quantifiers.

Let a $P = \{p_i; i = 1, \dots, N\}$ with $\sum_{i=1}^N p_i = 1$, be a discrete probability distribution, with N the number of possible states of the system under study. The Shannon's logarithmic information measure reads

$$S[P] = - \sum_{i=1}^N p_i \ln [p_i] . \quad (1)$$

If $S[P] = S_{\min} = 0$, we are in position to predict with complete certainty which of the possible outcomes i , whose probabilities are given by p_i , will actually take place. Our knowledge of the underlying process described by the probability distribution is maximal in this instance. In contrast, our knowledge is minimal for a uniform distribution $P_e = \{p_i = 1/N; i = 1, \dots, N\}$ since every outcome exhibits the same probability of occurrence, and the uncertainty is maximal, i.e., $S[P_e] = S_{\max} = \ln N$. These two situations are extreme cases, therefore we focus on the ‘normalized’ Shannon entropy, $0 \leq H \leq 1$, given as

$$H[P] = S[P]/S_{\max} . \quad (2)$$

Contrary to information content, there is no universally accepted definition of complexity. Here, we focus on describing the *complexity of time series* and do not refer to the complexity of the underlying *systems*. A complex system does not necessarily generate a complex output. In fact, “simple” models might generate complex data, while “complicated” systems might produce output data of low complexity [23].

An intuitive notion of a quantitative complexity attributes low values both to perfectly ordered data (i.e. with vanishing Shannon entropy) as well as to uncorrelated random data (with maximal Shannon entropy). For example, the statistical complexity of a simple oscillation or trend (ordered), but also of uncorrelated white noise (unordered) would be classified as low. Between the two cases of minimal and maximal entropy, data are more difficult to characterize and hence the complexity should be higher. We seek some functional

$C[P]$ quantifying structures present in the data which deviate from these two cases. These structures relate to organization, correlational structure, memory, regularity, symmetry, patterns, and other properties [24].

One would like to assume that the degree of correlational structures would be adequately captured by some functional $C[P]$ in the same way that Shannon's entropy $S[P]$ [22] "captures" randomness. Clearly, the ordinal structures present in a process is not quantified by randomness measures, and consequently, measures of statistical or structural complexity are necessary for a better understanding (characterization) of the system dynamics represented by their time series [25].

A suitable measure of complexity can be defined as the product of a measure of information and a measure of disequilibrium, i.e. some kind of distance from the equiprobable distribution of the accessible states of a system. In this respect, Rosso and coworkers [26] introduced an effective *Statistical Complexity Measure* (SCM) C , that is able to detect essential details of the dynamical processes underlying the dataset. Based on the seminal notion advanced by López-Ruiz *et al.* [27], this statistical complexity measure[28,26] is defined through the functional product form

$$C[P] = Q_J[P, P_e] \cdot H[P] \quad (3)$$

of the normalized Shannon entropy H , see eq. (2), and the disequilibrium Q_J defined in terms of the Jensen-Shannon divergence $J[P, P_e]$. That is,

$$Q_J[P, P_e] = Q_0 J[P, P_e] = Q_0 \{S[(P + P_e)/2] - S[P]/2 - S[P_e]/2\}, \quad (4)$$

the above-mentioned Jensen-Shannon divergence and Q_0 , a normalization constant such that $0 \leq Q_J \leq 1$:

$$Q_0 = -2 \left\{ \frac{N+1}{N} \ln(N+1) - \ln(2N) + \ln N \right\}^{-1}, \quad (5)$$

are equal to the inverse of the maximum possible value of $J[P, P_e]$. This value is obtained when one of the components of P , say p_m , is equal to one and the remaining p_j are zero.

The Jensen-Shannon divergence, which quantifies the difference between probability distributions, is especially useful to compare the symbolic composition between different sequences [29]. Note that the above introduced SCM depends on two different probability distributions: one associated with the system under analysis, P , and the other with the uniform distribution, P_e . Furthermore, it was shown that for a given value of H , the range of possible C values varies between a minimum C_{min} and a maximum C_{max} , restricting the possible values of the SCM [30]. Thus, it is clear that important additional information

related to the correlational structure between the components of the physical system is provided by evaluating the statistical complexity measure.

2.2 Determination of a probability distribution

The evaluation of the derived Information Theory quantifiers suppose some prior knowledge about the system; specifically for those previously introduced (Shannon entropy and statistical complexity), a probability distribution associated to the time series under analysis should be provided before. The determination of the most adequate PDF is a fundamental problem because the PDF P and the sample space Ω are inextricably linked.

Usual methodologies assign to each value of the series $X(t)$ (or non-overlapped set of consecutive values) a symbol from a finite alphabet $A = \{a_1, \dots, a_M\}$, thus creating a *symbolic sequence* that can be regarded to as a *non causal coarse grained* description of the time series under consideration. As a consequence, order relations and the time scales of the dynamics are completely lost.

Causal information may be duly incorporated if information about the past dynamics of the system is included in the symbolic sequence, i.e., symbols of alphabet A are assigned to a portion of the phase-space or trajectory. Bandt and Pompe (BP)[12] introduced a simple and robust symbolic methodology that takes into account time ordering of the time series by comparing neighboring values in a time series. The causality property of the PDF allows quantifiers (based on this PDFs) to discriminate between deterministic and stochastic systems [31]. The symbolic data are: (i) created by ranking the values of the series; and (ii) defined by reordering the embedded data in ascending order, which is equivalent to a phase space reconstruction with embedding dimension (pattern length) D and time lag τ . In this way, it is possible to quantify the diversity of the ordering symbols (patterns) derived from a scalar time series. Note that the appropriate symbol sequence arises naturally from the time series, and no model-based assumptions are needed. The procedure is the following:

- Given a series $\{x_t; t = 0, \Delta t, \dots, N\Delta t\}$, a sequence of vectors of length D is generated.

$$(s) \longmapsto (x_{t-(d-1)\Delta t}, x_{t-(d-2)\Delta t}, \dots, x_{t-\Delta t}, x_t) \quad (6)$$

Each vector turns out to be the “history” of the value x_t . Clearly, the longer the length of the vectors D , the more information about the history would the vectors have but a higher value of N is required to have an adequate statistics.

- The permutations $\pi = (r_0, r_1, \dots, r_{D-1})$ of $(0, 1, \dots, D-1)$ are called “order of patterns” of time t , defined by:

$$x_{t-r_{D-1}\Delta t} \leq x_{t-r_{D-2}\Delta t} \leq \dots \leq x_{t-r_1\Delta t} \leq x_{t-r_0\Delta t} \quad (7)$$

In order to obtain an unique result it is considered $r_i < r_{i-1}$ if $x_{t-r_i\Delta t} = x_{t-r_{i-1}\Delta t}$. In this way, all the $D!$ possible permutations π of order D , and the PDF $P = \{p(\pi)\}$ is defined as:

$$p(\pi) = \frac{\#\{s | s \leq N - D + 1; (s) \text{ has type } \pi\}}{N - D + 1} \quad (8)$$

In the last expression the $\#$ symbol denotes cardinality.

Thus, an ordinal pattern probability distribution $P = \{p(\pi_i), i = 1, \dots, D!\}$ is obtained from the time series. In this way the vector defined by eq. (8) is converted into a unique symbol π . We set $r_i < r_{i-1}$ if $x_{s-r_i} = x_{s-r_{i-1}}$ for uniqueness. The only condition for the applicability of the BP method is a very weak stationary assumption: for $k \leq D$, the probability for $x_t < x_{t+k}$ should not depend on t . Regarding the selection of the parameters, Bandt and Pompe suggested working with $3 \leq D \leq 6$ for typical time series lengths, and specifically considered a time lag $\tau = 1$ in their cornerstone paper.

Recently, the permutation entropy was extended to incorporate also amplitude information. Weighting the probabilities of individual patterns according to their variance alleviates potential issues regarding to ‘high noise, low signal’ patterns, because low-variance patterns that are strongly affected by noise are down-weighted in the resulting ‘weighted ordinal pattern distributions’. Hence, a potential disadvantage of ordinal pattern statistics, namely the loss of amplitude information, can be addressed by introducing weights in order to obtain a “weighted permutation entropy (WPE)” [19]. Non-normalized weights are computed for each temporal window for the time series X , such that

$$w_j = \frac{1}{D} \sum_{k=1}^D (x_{j+k-1} - \bar{X}_j^D)^2. \quad (9)$$

In the equation above $x_{j+k-1} - \bar{X}_j^D$ denotes the arithmetic mean of the current embedding vector of length D and its variance w_j is then used to weight the relative frequencies of each ordinal pattern p_j . Originally, this technique was proposed to discriminate patterns immersed in low noise. We take advantage of the fact that the fixed points are not computed in the WPE.

We calculated the normalized permutation Shannon entropy H and the statistical complexity C from these PDFs, and the obtained values are denoted as:

- H_{hist} , is the normalized Shannon entropy applied to non-causal PDF P_{hist}

- H_{BP} , is the normalized Shannon entropy applied to causal PDF P_{BP}
- H_{BPW} , is the normalized Shannon entropy applied to causal PDF with amplitude contribution P_{BPW}
- C_{BP} , is the normalized statistical complexity applied to causal PDF P_{BP}
- C_{BPW} , is the normalized statistical complexity applied to causal PDF with amplitude contribution P_{BPW}

2.3 Information Planes

A particularly useful visualization of the quantifiers from Information Theory is their juxtaposition in two-dimensional graphs. Four information planes are defined:

- (1) Causal entropy vs. non-causal entropy, $H_{BP} \times H_{hist}$
- (2) Causal entropy with amplitude contributions vs. non-causal entropy, $H_{BPW} \times H_{hist}$
- (3) Causal complexity vs. causal entropy, $C_{BP} \times H_{BP}$
- (4) Causal complexity with amplitude contributions vs. causal entropy with amplitude contributions, $C_{BPW} \times H_{BPW}$

These diagnostic tools were shown to be particularly efficient to distinguish between the deterministic chaotic and stochastic nature of a time series since the permutation quantifiers have distinct behaviors for different types of processes.

In fig. 1 we show the planes $H_{BP} \times H_{hist}$ and $H_{BPW} \times H_{hist}$ collapsed. In this plane a higher value in any of the entropies, H_{BP} , H_{BPW} or H_{hist} , implies an more uniformity of the involved PDF. The point $(1, 1)$ represents the ideal case with uniform histogram and uniform distribution of ordering patterns. We show some relevant points as example.

Ideal white random with uniform distribution gives a point at $(H_{hist}, H_{BP}) = (1, 1)$ represented by a blue circle, a red circle in the same position shows the results when amplitude contributions are included $(H_{hist}, H_{BPW}) = (1, 1)$. If we sort the vector generated by ideal white random generator in ascendant way, resulting points are shown by a blue square $(H_{hist}, H_{BP}) = (1, 0)$ and a red square $(H_{hist}, H_{BPW}) = (1, 0)$, this example illustrate the complementary of H_{hist} and H_{BP} .

Blue and red stars show (H_{hist}, H_{BP}) and (H_{hist}, H_{BPW}) respectively applied to a sawtooth signal. Values are perfectly distributed in all interval but only a few ordering patterns appear, this explains the high H_{hist} and low H_{BP} . The frequency of occurrence of low amplitude patterns is higher than high amplitude patterns, then the PDF with amplitude contributions is more uniform

and H_{BPW} is a little higher than H_{BP} . When sawtooth signal is contaminated with white noise H_{BP} and H_{BPW} are increased as shown with blue and red triangles. Clearly, new ordering patterns appear and both H_{BP} and H_{BPW} show higher values than non-contaminated case, however the growth of H_{BPW} is smaller than H_{BP} showing that the technique of recording amplitude contributions adds some immunity to noise.

Finally, we evaluated the quantifiers for a sequence of a logistic map that converges to a fixed point, in all the cases the length of data vector remains constant and the length of transitory is variable. Results obtained without amplitude contributions are depicted in blue dots, they converge to $(H_{hist}, H_{BP}) = (0, 0)$ as the length of transitory is shorter, however H_{BPW} (in red points) remains constant for all the cases. The last point in $(H_{hist}, H_{BP}) = (0, 0)$ corresponds to a vector of zeros, in this case the histogram of ordering patterns with amplitude contributions is also a zero vector and H_{BPW} can not be calculated. Through this last example, we show that the convergence to a fixed point can be detected by the joint information of H_{BP} and H_{BPW} .

In Figure 2 we show the causality plane $H_{BP} \times C_{BP}$. We can see that not the entire region $0 < H_{BP} < 1, 0 < C_{BP} < 1$ is achievable, in fact, for any PDF the pairs (H, C) of possible values fall between two extreme curves in the plane $H_{BP} \times C_{BP}$ [32]. Chaotic maps have intermediate entropy H_{BP} , while their complexity C_{BP} reaches larger values, very close to those of the upper complexity limit [13,33]. For regular processes, entropy and complexity have small values, close to zero. Uncorrelated stochastic processes are located in the planar location associated with H_{BP} near one and C_{BP} near zero. Ideal random systems having uniform Bandt & Pompe PDF, are represented by the point $(1, 0)$ [34] and a delta-like PDF corresponds to the point $(0, 0)$. In Fig. 2 we show $H_{BP} \times C_{BP}$ with and without amplitude contributions. The same sample points are showed to illustrate the planar positions for different data vectors.

In both information planes $H_{BP} \times H_{hist}$ in Fig. 1 and $H_{BP} \times C_{BP}$ in Fig. 2, stochastic, chaotic and deterministic data are clearly localized at different planar positions.

We also used the number of missing patterns MP as a quantifier [21]. As shown recently by Amigó *et al.* [35,36,37,38], in the case of deterministic maps, not all the possible ordinal patterns can be effectively materialized into orbits, which in a sense makes these patterns missing. Indeed, the existence of these missing ordinal patterns becomes a persistent fact that can be regarded as a new dynamical property. Thus, for a fixed pattern-length (embedding dimension D) the number of missing patterns of a time series (unobserved patterns) is independent of the series length N . Remark that this independence does not characterize other properties of the series such as proximity and correlation,

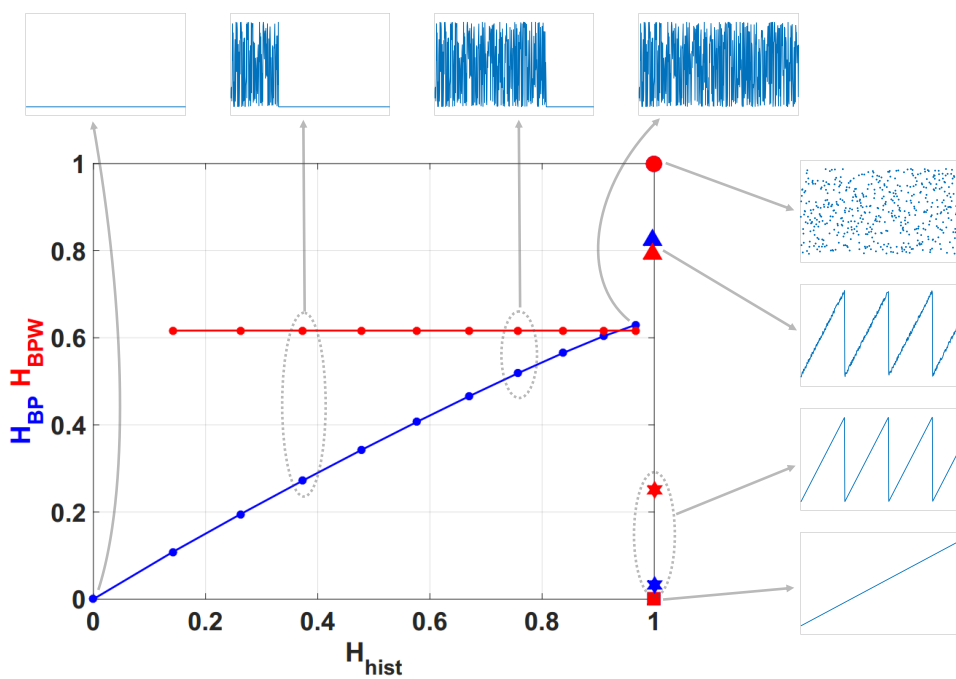


Figure 1. Causal-Non causal Entropy plane.

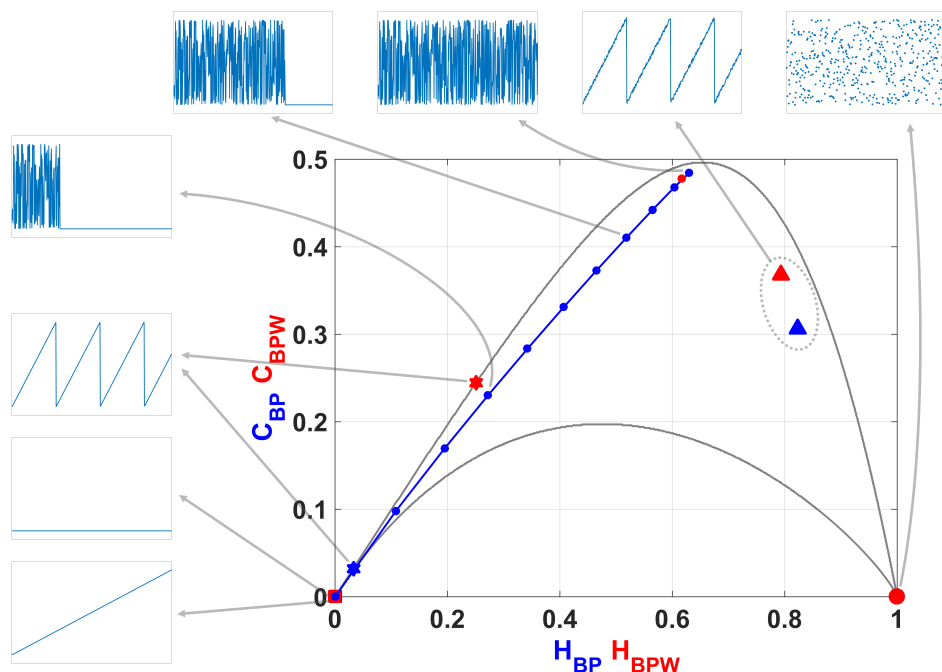


Figure 2. Causal Entropy-Complexity plane.

which die out with time [36,38].

A full discussion about the convenience of using these quantifiers is out of the scope of this work. Nevertheless reliable bibliographic sources do exist [15,17,21,27,30,39,40].

3 Results

Five pseudo chaotic maps were studied, two simple maps and three combination of them. For each one we have used numbers represented by floating-point (80 bits of mantissa) and fixed-point numbers with $1 \leq B \leq 53$, where B is the number of bits that represents the fractional part. Time series were generated using 100 randomly chosen initial conditions within their attraction domain (interval $[0, 1]$), for each one of these 54 number precisions.

The studied maps are logistic (LOG), tent (TENT), sequential switching between TENT and LOG (SWITCH) and skipping discarding the values in the odd positions (EVEN) or the values in the even positions (ODD) respectively.

Logistic map is interesting because is representative of the very large family of quadratic maps. Its expression is:

$$x_{n+1} = 4x_n(1 - x_n) \quad (10)$$

with $x_n \in \mathbb{R}$.

Note that to effectively work in a given representation it is necessary to change the expression of the map in order to make all the operations in the chosen representation numbers. For example, in the case of LOG the expression in binary fixed-point numbers is:

$$x_{n+1} = 4\epsilon \text{ floor} \left\{ \frac{x_n(1 - x_n)}{\epsilon} \right\} \quad (11)$$

with $\epsilon = 2^{-B}$ where B is the number of bits that represents the fractional part.

The Tent map has been extensively studied in the literature because theoretically it has nice statistical properties that can be analytically obtained. For example it is easy to proof that it has a uniform histogram and consequently an ideal $H_{hist} = 1$. The Perron-Frobenius operator and its corresponding eigenvalues and eigenfunctions may be analytically obtained for this map [41].

Tent map is represented with the equation:

$$x_{n+1} = \begin{cases} 2x_n & , \text{if } 0 \leq x_n \leq 1/2 \\ 2(1-x_n) & , \text{if } 1/2 < x_n \leq 1 \end{cases} \quad (12)$$

with $x_n \in \mathbb{R}$.

In base-2 fractional numbers rounding, equation (12) becomes:

$$x_{n+1} = \begin{cases} 2x_n & , \text{if } 0 \leq x_n \leq 1/2 \\ \epsilon \text{ floor}\left\{\frac{2 - 2x_n}{\epsilon}\right\} & , \text{if } 1/2 < x_n \leq 1 \end{cases} \quad (13)$$

with $\epsilon = 2^{-B}$.

Switching, even skipping and odd skipping procedures are shown in Fig. 3.

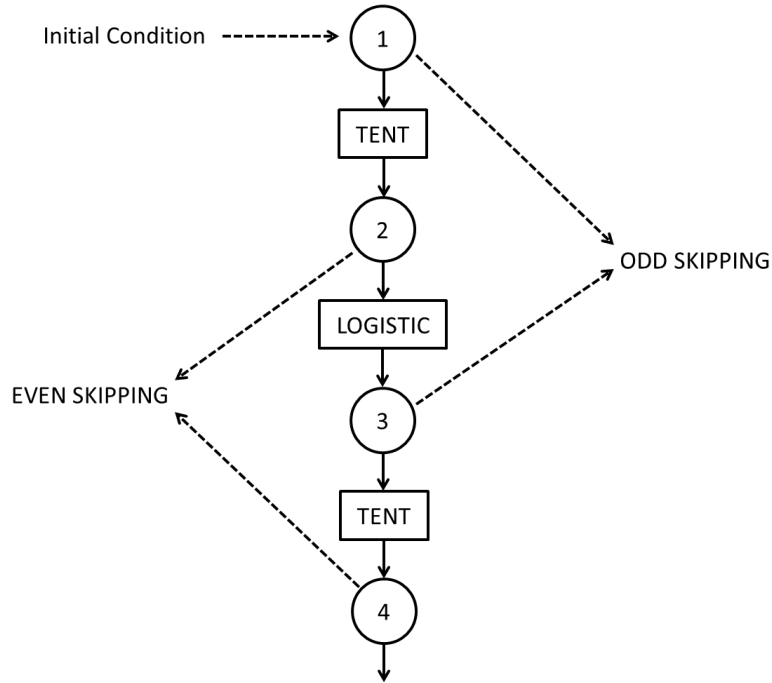


Figure 3. Sequential switching between Tent and Logistic maps. In the figure are also shown even and odd skipping strategies.

SWITCH map is expressed as:

$$\begin{cases} x_{n+1} = \begin{cases} 2x_n & , \text{if } 0 \leq x_n \leq 1/2 \\ 2(1-x_n) & , \text{if } 1/2 < x_n \leq 1 \end{cases} \\ x_{n+2} = 4x_{n+1}(1-x_{n+1}) \end{cases} \quad (14)$$

with $x_n \in \mathbb{R}$ and n an even number.

Skipping is a usual randomizing technique that increases the mixing quality of a single map and correspondingly increases the value of H_{BP} and decreases C_{BP} of the time series. Skipping does not change the values of H_{hist} for ergodic maps because it is evaluated using the non causal PDF (normalized histogram of values) [15].

In the case under consideration we study even and odd skipping of the sequential switching of Tent and Logistic maps:

- (1) Even skipping of the sequential switching of Tent and Logistic maps (EVEN).
If $\{x_n; n = 1, \dots, \infty\}$ is the time series generated by eq. (14), discard all the values in odd positions and retain the values in even positions.
- (2) Odd skipping of the sequential switching of Tent and Logistic maps. If $\{x_n; n = 1, \dots, \infty\}$ is the time series generated by eq. (14), discard all the values in even positions and retain all the values in odd positions.

Even skipping may be expressed as the composition function TENT \circ LOG while odd skipping may be expressed as LOG \circ TENT. The evolution of period as function of precision was reported in [1].

Let us detail our results for each of these maps.

3.1 Period T as a function of B

Grebogi and coworkers [7] have studied how the period T is related with the precision. There they saw that the period T scales with roundoff ϵ as $T \sim \epsilon^{-d/2}$ where d is the correlation dimension of the chaotic attractor.

Nagaraj *et al.* [1] studied the case of switching between two maps. They saw that the period T of the compound map obtained by switching between two chaotic maps is higher than the period of each map and they found that a random switching improves the results. Here we have considered sequential switching to avoid the use of another random variable, because it can include its own statistical properties in the time series.

Fig. 4 shows T vs. B in semi logarithmic scale. The experimental averaged points can be fitted by a straight line expressed as $\log_2 T = mB + b$ where m is the slope and b is the y -intercept. Results for all considered maps are summarized in Table 1.

Results are compatible for those obtained in [1]. Switching between maps increases the period T but skipping procedure decreases by almost half.

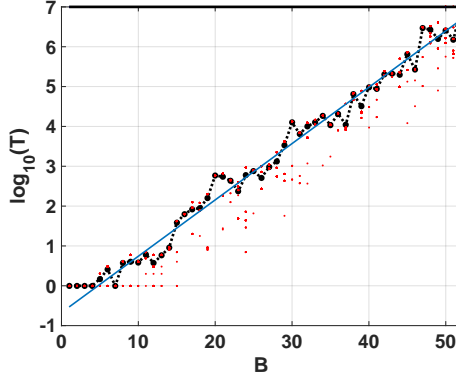


Figure 4. Period as function of precision in binary digits

Table 1
Period T as a function of B for the maps considered

map	m	b
TENT	0	0
LOG	0.139	-0.6188
SWITCH	0.1462	-0.5115
EVEN	0.1447	-0.7783
ODD	0.1444	-0.7683

3.2 Quantifiers of simple maps

Here we report our results for both simple maps, LOG and TENT

3.2.1 LOG

Figs. 5a to 5f show the statistical properties of LOG map in floating-point and fixed-point representation. All these figures show: 100 red points for each fixed-point precision ($1 \geq B \geq 53$) and in black their average (dashed black line connecting black dots), 100 horizontal dashed blue lines that are the results of each run in floating-point and a black solid line their average. Note that these lines are independent of x-axis. In this case, all the lines of the floating-point are overlapped.

According as B grows, statistical properties vary until they stabilize. For $B \geq 30$ the value of H_{hist} remains almost identical to the value for the floating-point representation whereas H_{BP} and C_{BP} stabilizes at $B > 21$. Their values are: $\langle H_{hist} \rangle = 0.9669$; $\langle H_{BP} \rangle = 0.6269$; $\langle C_{BP} \rangle = 0.4843$. Note that the stable value

of missing patterns $MP = 645$ makes the optimum $H_{BP} \leq \ln(75)/\ln(720) \simeq 0.65$. Then, $B = 30$ is the most convenient choice for hardware implementation because an increase in the number of fractional digits does not improve the statistical properties.

Some conclusions can be drawn regarding BP and BPW quantifiers. For $B = 1, 2, 3$ and 4 , the averaged BP quantifiers are almost 0 while the averaged BPW quantifiers can not be calculated (see in Figs. 5c and 5e the missing black dashed line). This is because for those sequences were the initial condition were 0 all iterations result to be a sequence of zeros (the fixed point of the map), this is more likely to happen when using small precisions because of roundoff.

When B increases the initial conditions are rounded to zero less frequently, this can be seen for $B > 6$. In this, case the generated sequences starting from a non-null value fall to zero after a short transitory very often. An interesting issue in Figs. 5c and 5e, is that BPW quantifiers show a high dispersion unlike BP quantifiers. This is because BPW procedure takes into account the transient and discards fixed points, unlike BP procedure considers all the values of the sequence. We can see in Figs. 5c and 5e for $1 < B < 10$ horizontal lines of red points that do not appear in Figs. 5b and 5d, this evidences that different initial conditions fall to the same orbits, even for adjacent precisions.

The same results are shown in double entropy planes with the precision as parameter (Fig. 6a without amplitude contributions and Fig. 6b with amplitude contributions). These figures show: 100 red points for each fixed-point precision (B) and their average in black (dashed black line connecting black dots), 100 blue dots that are the results of each run in floating-point and the black star is their average. Here, the 100 blue points and their average are overlapped.

As expected, the fixed-point architecture implementation converges to the floating-point value as B increases. For both planes, $H_{hist} \times H_{BP}$ and $H_{hist} \times H_{BPW}$, from $B = 20$, H_{hist} increases but H_{BP} and H_{BPW} remain constant. It can be seen that the distribution of values reaches high values ($\langle H_{hist} \rangle = 0.9669$) but their mixing is poor ($\langle H_{BP} \rangle = 0.6269$).

In Fig. 7a and 7b we show the entropy-complexity planes. Dotted grey lines are the upper and lower margins, it is expected that a chaotic system remains near the upper margin. These results characterize a chaotic behavior, in $H_{BP} \times C_{BP}$ plane we can see a low entropy and high complexity.

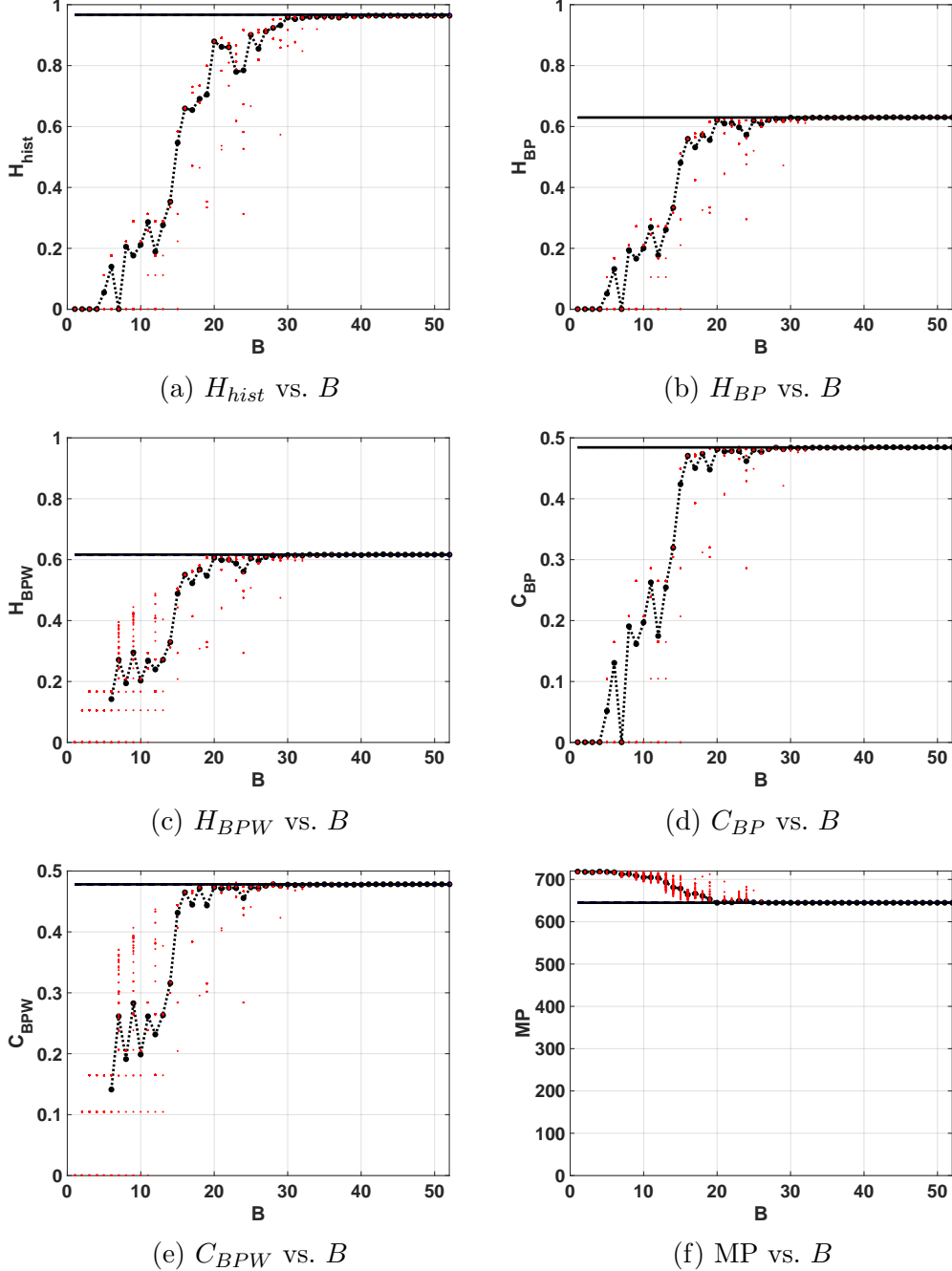


Figure 5. Statistical properties for LOG map as function of B

3.2.2 TENT

When this map is implemented in a computer using any numerical representation system (even floating-point!) truncation errors rapidly increase and make unstable fixed point in $x^* = 0$ to become stable. The sequences within the attractor domain of this fixed point will have a short transitory of length between 0 and B followed by an infinite number of 0's [42,43]. This issue is easily

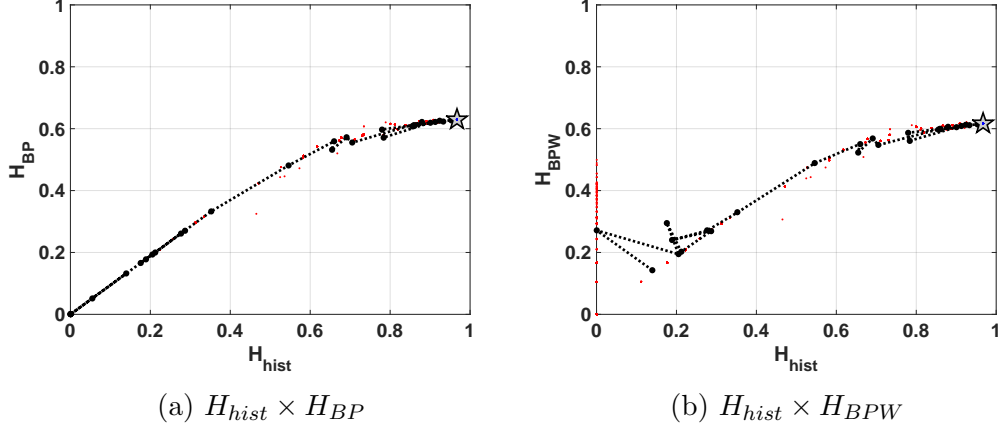


Figure 6. Evolution of statistical properties in double entropy plane for LOG map

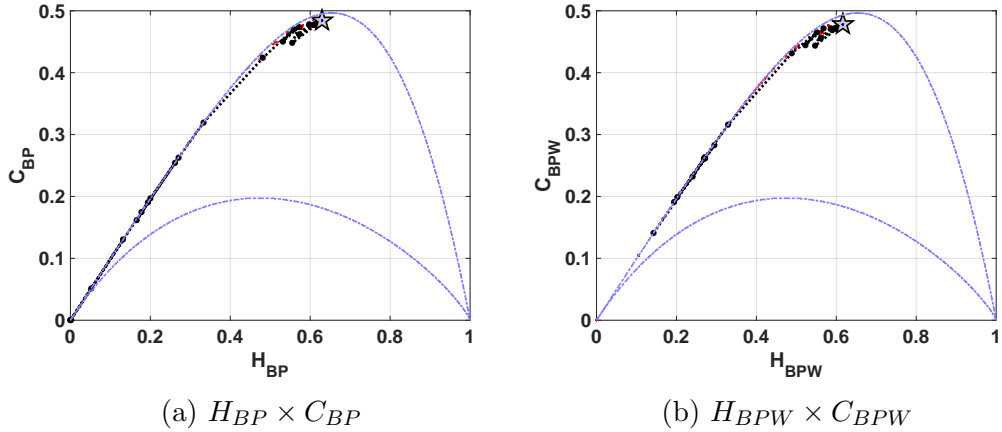


Figure 7. Evolution of statistical properties in causal entropy-complexity plane for LOG map

explained in [44], the problem appears because all iterations have a left-shift operation that carries the 0's from the right side of the number to the most significant positions.

Figs. 8a to 8f show the quantifiers for floating- and fixed-point numerical representations. H_{hist} , H_{BP} and C_{BP} quantifiers are equal to zero for all precisions, this reflects that the series quickly converge toward a fixed point for every initial conditions. In the case of H_{BPW} and C_{BPW} quantifiers are different to zero because BPW procedure discards the elements once the fixed point is reached. The high dispersions in H_{BPW} , C_{BPW} and MP are related to the short length of serie's transient. These transients that converge to a fixed point have a maximum length of B elements (iterations) for fixed-point arithmetic and 80 for floating-point (long double precision).

Summarizing, in spite of using a high number of bits (with any 2-based numerical representation) to represent the digitalized TENT map it always converges

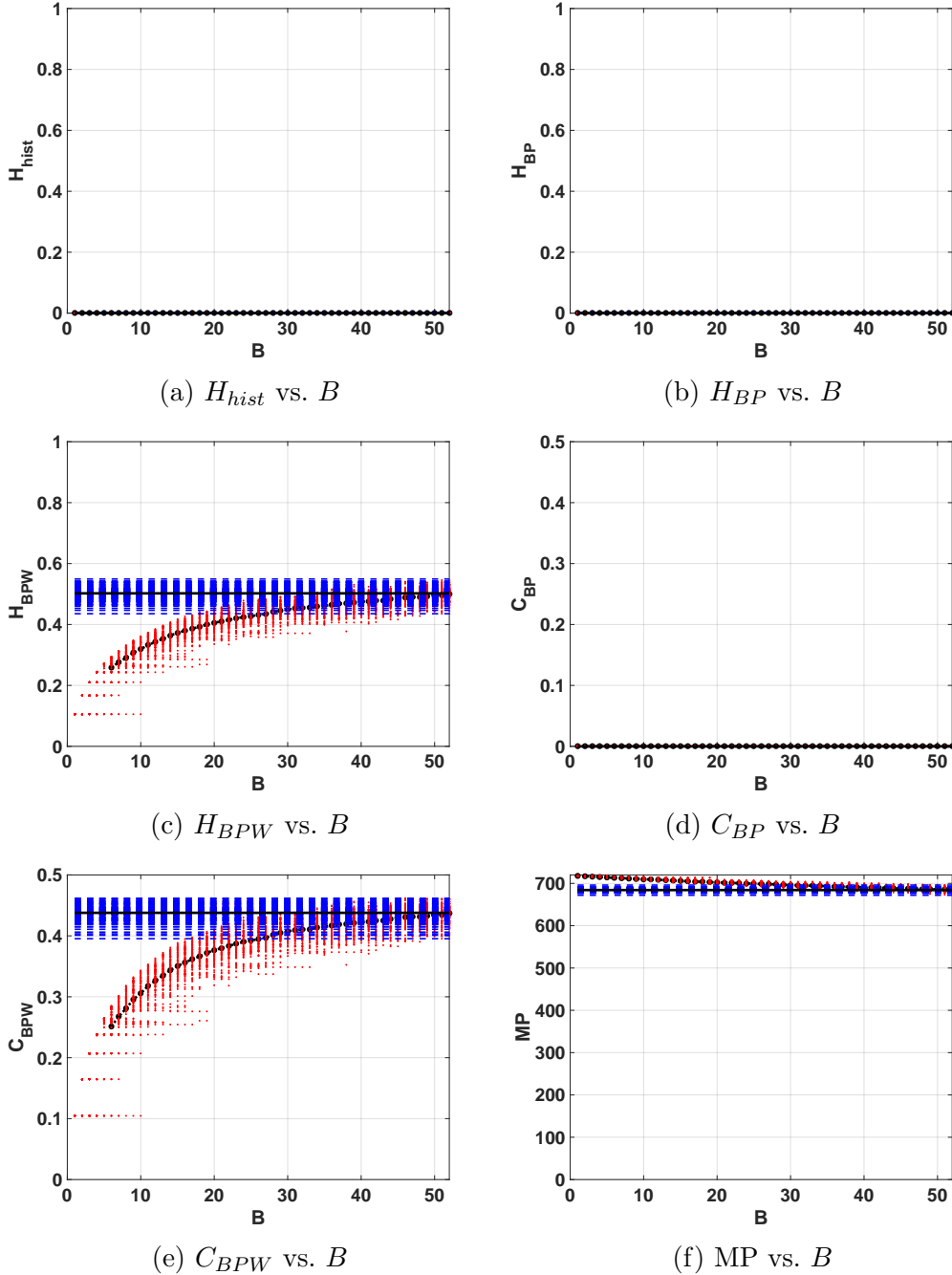


Figure 8. Statistical properties of TENT map quickly to the fixed point in $(x_n, x_{n+1}) = (0, 0)$.

3.3 Quantifiers of combined Maps

Here we report our results for the three combinations of the simple maps, SWITCH, EVEN and ODD.

3.3.1 SWITCH

Results with sequential switching are shown in Figs. 9a to 9f. The calculated entropy value for floating-point implementation is $\langle H_{hist} \rangle = 0.9722$, this value is slightly higher than the one obtained for the LOG map. For fixed-point arithmetic this value is reached in $B = 24$, but it stabilizes from $B = 28$. Regarding the ordering patterns the number of MP decreases to 586, this value is lower than the one obtained for LOG map. It means the entropy H_{BP} may increase up to $\ln(134)/\ln(720) \simeq 0.74$. BP and BPW quantifiers reach their maximum of $\langle H_{BP} \rangle = 0.6546$ and $\langle H_{BPW} \rangle = 0.6313$ at $B = 16$, but they stabilize from $B = 24$. Complexities are lower than for LOG, $\langle C_{BP} \rangle = 0.4580$ and $\langle C_{BPW} \rangle = 0.4578$, these values are reached for $B \geq 15$ but they stabilize for $B \geq 23$. Compared with LOG, statistical properties are better with less amount of bits, for $B \geq 24$ this map reaches optimal characteristics in the sense of random source.

Furthermore, we encountered one initial condition in floating-point long double precision with an anomalous behavior Figs. 9a, 9b and 9d show an horizontal blue dashed line that is far from the average value, unlike this is not detected by quantifiers based on *BPW* procedure in Figs. 9c and 9e. Nevertheless comparing both procedures (*BP* and *BPW*) we were able to detect a falling to fixed point after a long transitory, the *BPW* procedure discards the constant values (corresponding with a fixed point) and works only over the transitory values.

Double entropy plane $H_{hist} \times H_{BP}$ is showed in Fig. 10. The reached point in this plane for SWITCH map is similar to that reached for LOG map, and it is denoted by a star in the figure. The mixing is slight better in this case.

Entropy-complexity plane $H_{BP} \times C_{BP}$ is showed in Fig. 11. If we compare with the same plane in the case of LOG (Fig. 7a), C_{BP} is lower for SWITCH, this fact shows a more random behavior.

3.3.2 EVEN and ODD

In Figs. 12a and 13a we can see that quantifiers related to the normalized histogram of values slightly degrades with the skipping procedure. For example $\langle H_{hist} \rangle$ reduces from 0.9722 without skipping to 0.9459 for EVEN and 0.9706 for ODD. This difference between EVEN and ODD in floating point is because a high dispersion was obtained for H_{hist} , H_{BP} and C_{BP} but not for H_{BPW} or C_{BPW} .

Figures 12b to 12f and Figs. 13b to 13f show the results of BP and BPW quantifiers for EVEN and ODD respectively. Higher accuracy is required to achieve lower complexity than without using skipping. From the MP point of

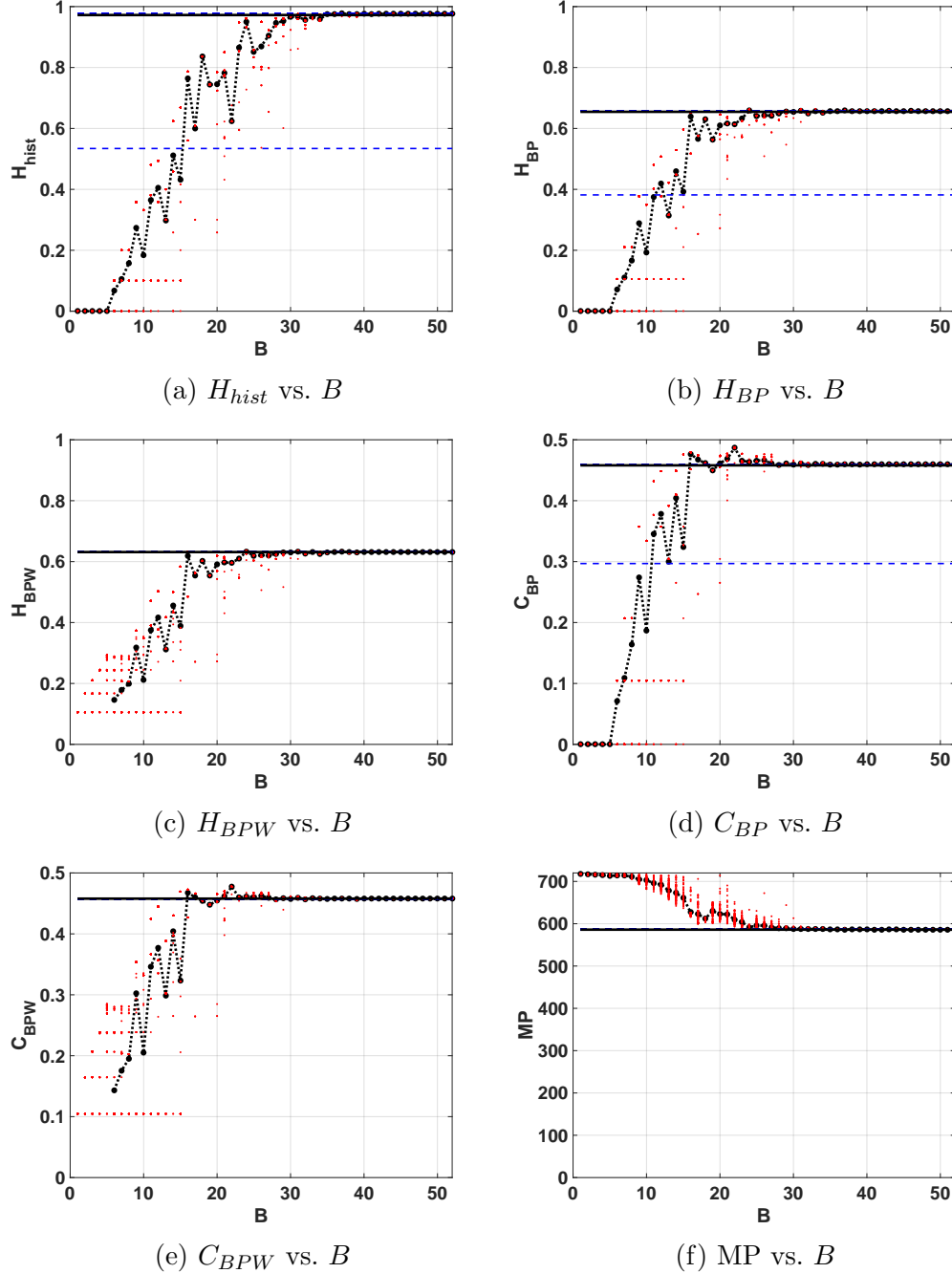


Figure 9. Statistical properties of SWITCH map

view a great improvement is obtained using any of the skipping strategies but ODD is slightly better than EVEN. Missing patterns are reduced to $MP = 118$ for EVEN and ODD, increasing the maximum allowed Bandt & Pompe entropy that reaches the mean value $\langle H_{BP} \rangle = 0.8381$ for EVEN, and $\langle H_{BP} \rangle = 0.9094$. The complexity is reduced to $\langle C_{BP} \rangle = 0.224$ for EVEN and $\langle C_{BP} \rangle = 0.282$ for ODD. The minimum number of bits to converge to this value is $B > 40$ for both EVEN and ODD maps.

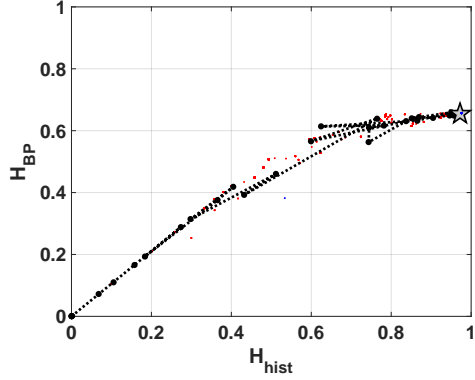


Figure 10. Evolution of statistical properties in double entropy plane for SWITCH map $H_{hist} \times H_{BP}$.

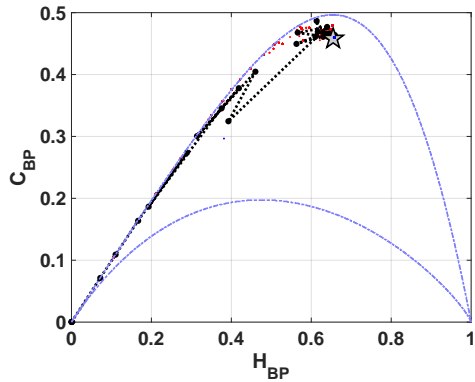


Figure 11. Evolution of statistical properties in causal entropy-complexity plane for SWITCH map $H_{BP} \times C_{BP}$.

The enhancement showed in Fig. 12 and 13 is reflected in the position of asymptotic point in the planes 14, and 15. In both cases this position is closest to the ideal point $(H_{hist}, H_{BP}) = (1, 1)$, because the resulting vectors present better mixing.

Compatible results are shown in Figs. 16 and 17, the position of asymptotic point is closest to the ideal point $(H_{hist}, H_{BP}) = (1, 0)$. This result reflects that mixing is better because the complexity of resulting system is lower. This plane detects that the vector generated by ODD skipping is more mixed than EVEN.

4 Conclusions

In this paper we explored the statistical degradation of simple, switched and skipped chaotic maps due to the inherent error of a based-2 systems. We evaluated mixing and amplitude distributions from a statistical point of view.

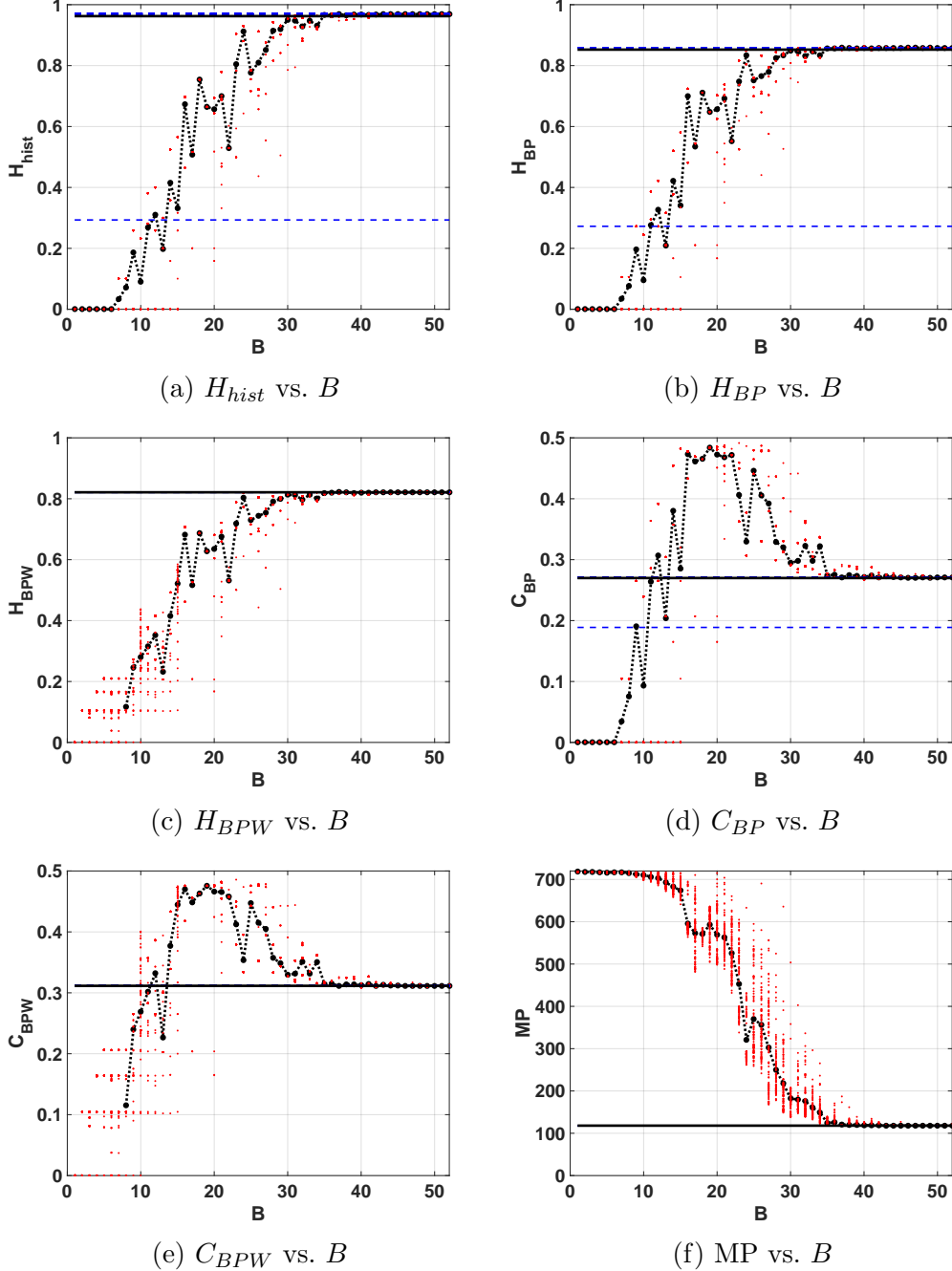


Figure 12. Statistical properties of EVEN map

Our work complements previous results given in [1], where period lengths were investigated. In that sense, our results were compatible with these. We can see that the switching between two maps increases the dependence of period as function of precision, this is because the correlation length is also increased. Nevertheless, the standard procedure of skipping reduce the period length in almost a half.

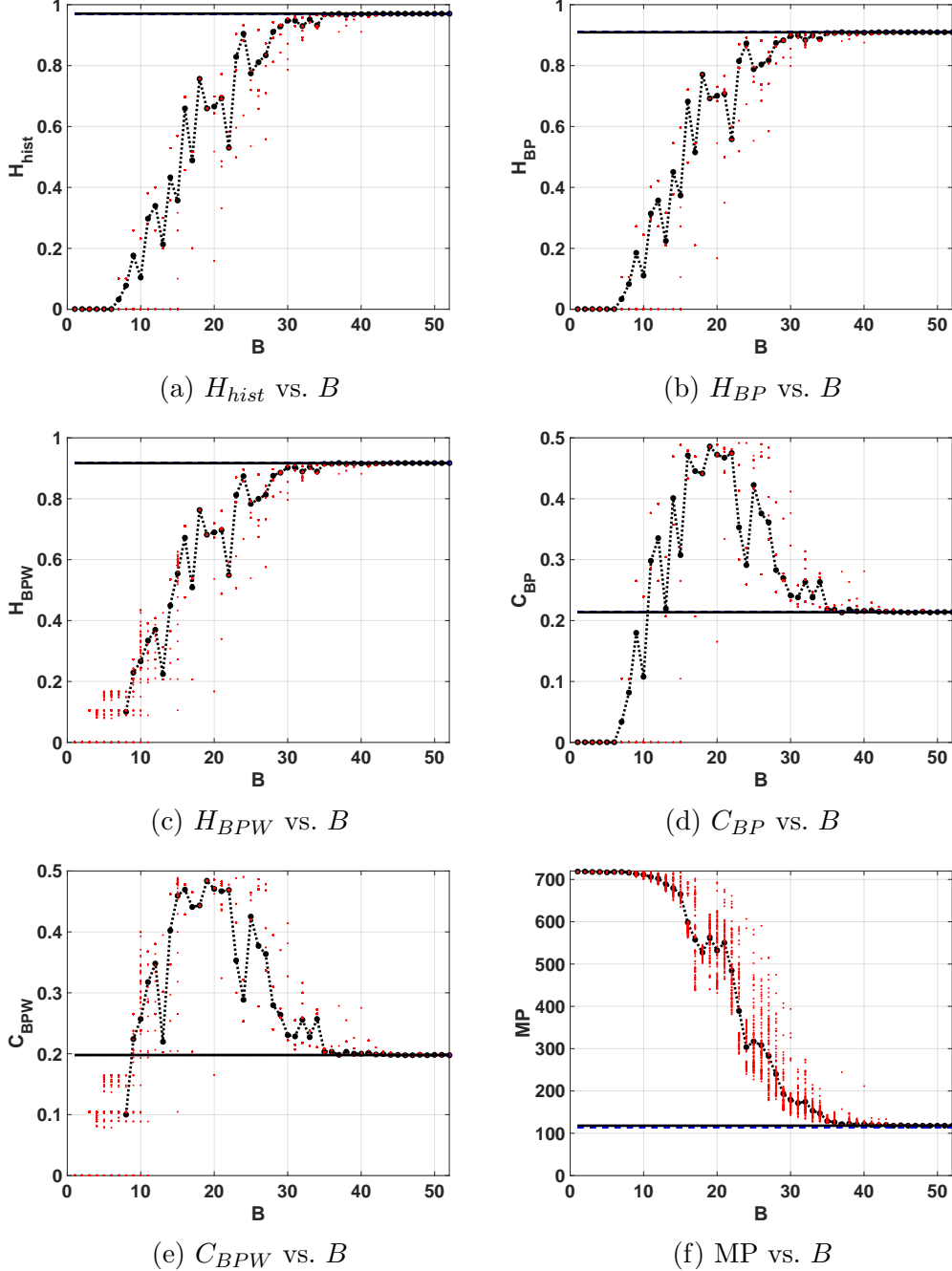


Figure 13. Statistical properties of ODD map

All statistics of the maps represented in fixed-point produces a non-monotonous evolution toward the floating-point results. This result is relevant because it shows that increasing the precision is not always recommended.

It is specially interesting to note that some systems (TENT) with very nice statistical properties in the real numbers world, become “pathological” when binary numerical representations are used. As a rule, if a map is generated

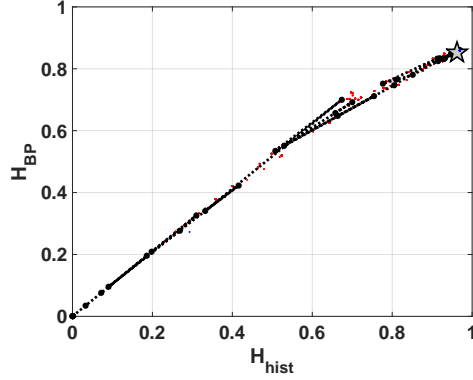


Figure 14. Evolution of statistical properties in double entropy plane for EVEN map $H_{hist} \times H_{BP}$.

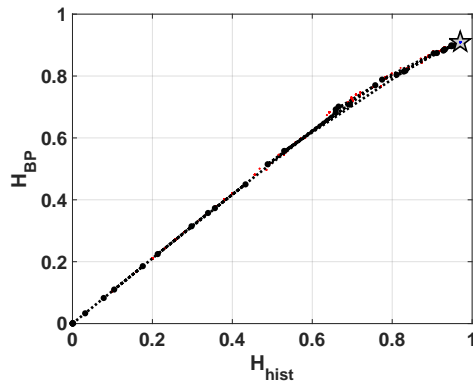


Figure 15. Evolution of statistical properties in double entropy plane for ODD map $H_{hist} \times H_{BP}$.

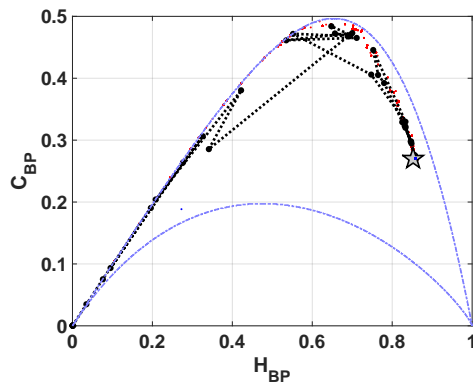


Figure 16. Evolution of statistical properties in entropy-complexity plane for EVEN map $H_{BP} \times C_{BP}$.

only by shift operations (it depends on the base of the arithmetic logic unit and the map itself), all initial conditions will converge to a fixed point with a transient no longer than the length of the mantissa being used.

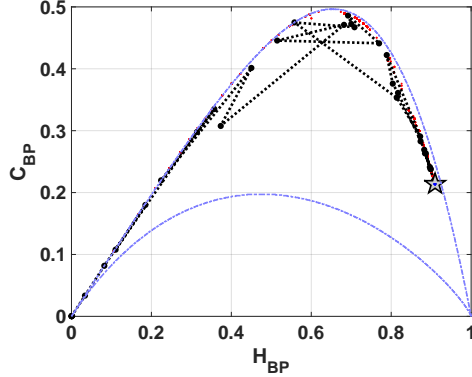


Figure 17. Evolution of statistical properties in entropy-complexity plane for ODD map $H_{BP} \times C_{BP}$.

By comparing between BP and BPW quantifiers, we were able to detect falls to fixed points and to estimate the relative length of transient. It can be seen in all implementations of TENT, in one initial condition of SWITCH and EVEN for floating-point implementation.

Related to statistical behavior, our results show that SWITCH has a marginal improvement in the mixing with respect to LOG (and TENT, of course). However the greatest improvement comes when skipping is applied, we can see that BP and BPW entropies grow and BP and BPW complexities decrease, for the same numerical representation. This result is relevant because evidences that a long period is not synonymous of good statistics, switched maps EVEN and ODD have half period lengths but their mixing is better and their amplitude distributions remain almost equal. As counterpart, more precision is needed to reach the better asymptotes that offers the switching method.

Acknowledgment

This work was partially supported by the Consejo Nacional de Investigaciones Científicas y Técnicas (CONICET), Argentina (PIP 112-201101-00840), UNMDP and the International Centre for Theoretical Physics (ICTP) Associate-ship Scheme.

References

- [1] N. Nagaraj, M. C. Shastry, and P. G. Vaidya. Increasing average period lengths by switching of robust chaos maps in finite precision. *The European Physical Journal Special Topics*, 165(1):73–83, dec 2008.

- [2] Pedro María Alcover. Moiré interferences in the map of orbits of the Mandelbrot Set. *Commun. Nonlinear Sci. Numer. Simul.*, 42:545–559, jan 2017.
- [3] S P Dias, L Longa, and E Curado. Influence of the finite precision on the simulations of discrete dynamical systems. *Commun. Nonlinear Sci. Numer. Simul.*, 16:1574–1579, 2011.
- [4] Mohamed Salah Azzaz, Camel Tanougast, Said Sadoudi, and Ahmed Bouridane. Synchronized hybrid chaotic generators: Application to real-time wireless speech encryption. *Commun. Nonlinear Sci. Numer. Simul.*, 18(8):2035–2047, 2013.
- [5] William Graham Hoover and Kenichiro Aoki. Order and chaos in the one-dimensional 4 model: N-dependence and the Second Law of Thermodynamics. *Commun Nonlinear Sci Numer Simulat*, 49:192–201, 2017.
- [6] L De Micco, M Antonelli, and H.A. Larrondo. Stochastic degradation of the fixed-point version of 2D-chaotic maps. *Chaos, Solitons and Fractals*, 104:477–484, 2017.
- [7] Celso Grebogi, Edward Ott, and James A. Yorke. Roundoff-induced periodicity and the correlation dimension of chaotic attractors. *Physical Review A*, 38(7):3688–3692, oct 1988.
- [8] Xinzhi Liu, Kok-Lay Teo, Hongtao Zhang, and Guanrong Chen. Switching control of linear systems for generating chaos. *Fractals An Interdisciplinary Journal On The Complex Geometry Of Nature*, 30(3):725–733, nov 2006.
- [9] Emanuel Gluskin. The nonlinear-by-switching systems (a heuristic discussion of some basic singular systems). 2008.
- [10] D. G. Zarlenga, H. A. Larrondo, C. M. Arizmendi, and Fereydoon Family. Complex synchronization structure of an overdamped ratchet with discontinuous periodic forcing. *Physical Review E - Statistical, Nonlinear, and Soft Matter Physics*, 80(1):011127, jul 2009.
- [11] L De Micco, H A Larrondo, A Plastino, and O A Rosso. Quantifiers for randomness of chaotic pseudo-random number generators. *Philosophical transactions. Series A, Mathematical, physical, and engineering sciences*, 367(1901):3281–3296, aug 2009.
- [12] Christoph Bandt and Bernd Pompe. Permutation entropy: a natural complexity measure for time series. *Physical Review Letters*, 88(17):174102, apr 2002.
- [13] O. A. Rosso, H. A. Larrondo, M. T. Martín, A. Plastino, and M. A. Fuentes. Distinguishing Noise from Chaos. *Physical Review Letters*, 99(15):154102, oct 2007.
- [14] J. S.Armand Eyebe Fouda, Wolfram Koepf, and Sabir Jacquir. The ordinal Kolmogorov-Sinai entropy: A generalized approximation. *Commun. Nonlinear Sci. Numer. Simul.*, 46:103–115, 2017.
- [15] L. De Micco, C. M. González, H. A. Larrondo, M. T. Martín, A. Plastino, and O. A. Rosso. Randomizing nonlinear maps via symbolic dynamics. *Physica A: Statistical Mechanics and its Applications*, 387(14):3373–3383, jun 2008.

- [16] Luciana De Micco, Juana Graciela Fernández, Hilda A. Larrondo, Angelo Plastino, and Osvaldo A. Rosso. Sampling period, statistical complexity, and chaotic attractors. *Physica A: Statistical Mechanics and its Applications*, 391(8):2564–2575, apr 2012.
- [17] Osvaldo A Rosso, Luciana De Micco, Hilda A Larrondo, Maria T Martín, and Angelo Plastino. Generalized Statistical Complexity Measure. *International Journal Of Bifurcation And Chaos*, 20(03):775, mar 2010.
- [18] M Antonelli, L De Micco, and H Larrondo. Measuring the jitter of ring oscillators by means of information theory quantifiers. *Communications in Nonlinear Science and Numerical Simulation*, 43:139–150, 2017.
- [19] Bilal Fadlallah, Badong Chen, Andreas Keil, and José Príncipe. Weighted-permutation entropy: A complexity measure for time series incorporating amplitude information. *Physical Review E - Statistical, Nonlinear, and Soft Matter Physics*, 87(2):1–7, 2013.
- [20] José María Amigó, S Zambrano, and M. A. F Sanjuán. True and false forbidden patterns in deterministic and random dynamics. *Europhysics Letters (EPL)*, 79(5):50001, sep 2007.
- [21] O A Rosso, L C Carpi, P M Saco, M G Ravetti, H A Larrondo, and A Plastino. The Amigó paradigm of forbidden/missing patterns: A detailed analysis. *European Physical Journal B*, 85(12), 2012.
- [22] Claude Elwood Shannon and Warren Weaver. The mathematical theory of communication. *Bell System Technical Journal*, 27(3):379–423, 1948.
- [23] Holger Kantz, J. (Jürgen) Kurths, and G. (Gottfried) Mayer-Kress. *Nonlinear analysis of physiological data*. Springer, 1998.
- [24] David P. Feldman, Carl S. McTague, and James P. Crutchfield. The organization of intrinsic computation: Complexity-entropy diagrams and the diversity of natural information processing. *Chaos*, 18(4):043106, dec 2008.
- [25] David P Feldman and James P Crutchfield. Measures of statistical complexity: Why? *Physics Letters A*, 238(4-5):244–252, feb 1998.
- [26] P. W. Lamberti, M. T. Martín, A Plastino, and O. A. Rosso. Intensive entropic non-triviality measure. *Physica A: Statistical Mechanics and its Applications*, 334(1-2):119–131, mar 2004.
- [27] R. López-Ruiz, H. L. Mancini, and X. Calbet. A statistical measure of complexity. *Physics Letters A*, 209(5-6):321–326, dec 1995.
- [28] M. T. Martín, A Plastino, and O. A. Rosso. Statistical complexity and disequilibrium. *Physics Letters, Section A: General, Atomic and Solid State Physics*, 311(2-3):126–132, may 2003.
- [29] Ivo Grosse, Pedro Bernaola-Galván, Pedro Carpena, Ramón Román-Roldán, Jose Oliver, and H. Eugene Stanley. Analysis of symbolic sequences using the Jensen-Shannon divergence. *Physical Review E*, 65(4):041905, mar 2002.

- [30] M T Martín, A Plastino, and O A Rosso. Generalized statistical complexity measures: Geometrical and analytical properties. *Physica A: Statistical Mechanics and its Applications*, 369(2):439–462, 2006.
- [31] O. A. Rosso, L. Zunino, D. G. Pérez, A. Figliola, H. A. Larrondo, M. Garavaglia, M. T. Martín, and A. Plastino. Extracting features of Gaussian self-similar stochastic processes via the Bandt-Pompe approach. *Physical Review E - Statistical, Nonlinear, and Soft Matter Physics*, 76(6):061114, dec 2007.
- [32] C Anteneodo and A. R. Plastino. Some features of the López-Ruiz-Mancini-Calbet (LMC) statistical measure of complexity. *Physics Letters, Section A: General, Atomic and Solid State Physics*, 223(5):348–354, dec 1996.
- [33] Felipe Olivares, Angelo Plastino, and Osvaldo A. Rosso. Contrasting chaos with noise via local versus global information quantifiers. *Physics Letters A*, 376(19):1577–1583, apr 2012.
- [34] C. M. González, H. A. Larrondo, and O. A. Rosso. Statistical complexity measure of pseudorandom bit generators. *Physica A: Statistical Mechanics and its Applications*, 354(1-4):281–300, aug 2005.
- [35] José M. Amigó, Ljupco Kocarev, and Janusz Szccepanski. Order patterns and chaos. *Physics Letters, Section A: General, Atomic and Solid State Physics*, 355(1):27–31, jun 2006.
- [36] J M Amigó, L Kocarev, and I Tomovski. Discrete entropy. *Physica D: Nonlinear Phenomena*, 228(1):77–85, 2007.
- [37] J. M. Amigó, S. Zambrano, and M. A. F. Sanjuán. Combinatorial detection of determinism in noisy time series. *Europhysics Letters*, 83(6):60005, sep 2008.
- [38] José Amigó. *Permutation Complexity in Dynamical Systems*. Springer Series in Synergetics. Springer Berlin Heidelberg, Berlin, Heidelberg, 2010.
- [39] R. Wackerbauer, A. Witt, H. Atmanspacher, J. Kurths, and H. Scheingraber. A comparative classification of complexity measures. *Chaos, Solitons and Fractals*, 4(1):133–173, jan 1994.
- [40] O. A. Rosso, H. A. Larrondo, M. T. Martín, A. Plastino, and M. A. Fuentes. Distinguishing noise from chaos. *Physical Review Letters*, 99(15):154102, oct 2007.
- [41] Andrzej Lasota and Michael C. Mackey. *Chaos, fractals, and noise : stochastic aspects of dynamics*. Number 97. Springer-Verlag, 1994.
- [42] M. Jessa. The period of sequences generated by tent-like maps. *IEEE Transactions on Circuits and Systems I: Fundamental Theory and Applications*, 49(1):84–89, 2002.
- [43] Sergio Callegari, Gianluca Setti, and P.J. Langlois. A CMOS tailed tent map for the generation of uniformly distributed chaotic sequences. In *Proceedings of 1997 IEEE International Symposium on Circuits and Systems. Circuits and Systems in the Information Age ISCAS '97*, volume 2, pages 781–784. IEEE, 2013.

[44] Shujun Li. When Chaos Meets Computers, 2004.